Eur Biophys J (2007) 37:71–80
DOI 10.1007/s00249-007-0165-z

ORIGINAL PAPER

Helix orientations in membrane-associated Bcl-X_L determined by ^{15}N-solid-state NMR spectroscopy

Christopher Aisenbrey · U. S. Sudheendra · Helen Ridley · Philippe Bertani · Arnaud Marquette · Svetlana Nedelkina · Jeremy H. Lakey · Burkhard Bechinger

Received: 22 January 2007 / Revised: 22 March 2007 / Accepted: 31 March 2007 / Published online: 10 May 2007

Abstract Controlled cell death is fundamental to tissue hemostasis and apoptosis malfunctions can lead to a wide range of diseases. Bcl-x_L is an anti-apoptotic protein the function of which is linked to its reversible interaction with mitochondrial outer membranes. Its interfacial and intermittent bilayer association makes prediction of its bound structure difficult without using methods able to extract data from dynamic systems. Here we investigate Bcl-x_L associated with oriented lipid bilayers at physiological pH using solid-state NMR spectroscopy. The data are consistent with a C-terminal transmembrane anchoring sequence and an average alignment of the remaining helices, i.e. including helices 5 and 6, approximately parallel to the membrane surface. Data from several biophysical approaches confirm that after removal of the C-terminus from Bcl-x_L its membrane interactions are weak. In the presence of membranes Bcl-x_L can still interact with a Bak BH3 domain peptide suggesting a model where the hydrophobic C-terminus of the protein unfolds and inserts into the membrane. During this conformational change the Bcl-x_L hydrophobic binding pocket becomes accessible for protein–protein interactions whilst the structure of the N-terminal region remains intact.

Keywords Membrane protein structure · Oriented lipid bilayer · Helix tilt angle · Topology · Apoptosis · Cancer · Protein–protein interactions

Introduction

Apoptosis is the controlled elimination of cells, a strategy of regulation which must have evolved early since it is found in organisms as diverse as fruitflies, nematodes, mammals (Borner 2003) and even fungi (Phillips et al. 2006). Controlled cell death occurs in a wide variety of cells in both developing and adult organisms, including neuronal and colonic cell lines (Butler et al. 1999; Merry and Korsmeyer 1997). The Bcl-2 family of proteins is intrinsically related to the regulation of controlled cell death and malfunction can result in a variety of disorders including cancer, autoimmunity and neurodegeneration (Adams and Cory 2001; Chao and Korsmeyer 1998). Although there is an ongoing and unresolved debate about the details of how apoptotic control is exerted, it is certain that the Bcl-2 proteins are key players in the game.

Through the identification of four sequence homology domains (BH1–BH4, Fig. 1) at least three different subgroups have been identified within the Bcl-2 family. Whereas the BH1-4 proteins (including Bcl-x_L and Bcl-2)

Electronic supplementary material The online version of this article (doi:10.1007/s00249-007-0165-z) contains supplementary material, which is available to authorized users.

C. Aisenbrey · U. S. Sudheendra · P. Bertani · A. Marquette · S. Nedelkina · B. Bechinger
Institut de Chimie de Strasbourg, Université Louis Pasteur/CNRS LC3-UMR 7177, 4, rue Blaise Pascal, 67070 Strasbourg, France

Present Address:
C. Aisenbrey
Biofysikalisk Kemi Umeå Universitet,
90187 Umeå, Sweden

H. Ridley · J. H. Lakey
Institute for Cell and Molecular Biosciences,
The Medical School, The University of Newcastle-upon-Tyne,
NE2 4HH Newcastle, UK

B. Bechinger (✉)
Institut de Chimie, 4, rue Blaise Pascal,
67070 Strasbourg, France
e-mail: bechinger@chimie.u-strasbg.fr

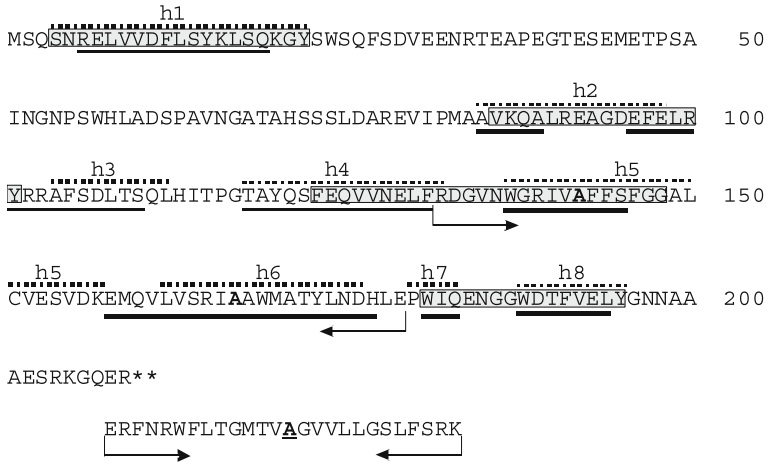

Fig. 1 The protein and peptide sequences investigated in this and other studies are indicated. The amino acid sequences of Bcl-x_L-ΔC (residues 1–209) as well as of the C-terminal region are shown as one-letter code (accession number Q07817). The helical regions observed in the X-ray crystallographic- or solution NMR structures of Bcl-x_L-ΔC are indicated by *hatched lines* and the helix number; those that are found in the presence of detergent micelles are labelled with *solid lines* (Losonczi et al. 2000; Muchmore et al. 1996). In *bold letters* are shown the alanine positions that have been selectively labelled with ^{15}N in the synthetic peptide 132–179, encompassing the helix5-loop–helix6 region, or in the peptide composed of residues 208–233, corresponding to the C-terminus. The delineations of these two peptides are shown by *arrows*. The BH4, BH3, BH1 and BH2 homology domains are indicated in *grey*

exhibit anti-apoptotic activity (pro-survival), those that lack the BH4 domain are pro-apoptotic (BH1-3, e.g. Bax). Furthermore, BH3-only proteins such as Bak exist and have pro-apoptotic activity (Borner 2003). The proteins form a complex interaction network where the activity is regulated by protein–protein and protein–membrane interactions concomitant with the re-localisation of the proteins from the cytoplasm to organellar membranes (Borner 2003). It is generally believed that targeting of Bax to the mitochondrial outer membrane and pore-formation is an important step during a cascade of regulatory interactions and events. Most members of the wider family of Bcl-2 proteins possess C-terminal hydrophobic anchor sequences, which facilitate their interaction with membranes.

The high-resolution structures of a number of members of the Bcl-2 family have been determined by X-ray diffraction and solution state NMR spectroscopy (Day et al. 2005; Huang et al. 2002, 2003; Muchmore et al. 1996). These include anti-apoptotic (Bcl-x_L, Bcl-2, Bcl-w, KSHV-Bcl-2, BHRF1, Mcl-1) as well as pro-apoptotic members of the family (Bax, Bid). The three-dimensional structures exhibit a hydrophobic helical hairpin in the centre of the fold, surrounded by a layer of amphipathic helices on each side of the resulting 'sandwich' (Petros et al. 2004). This motif has also been observed for channel-forming bacterial toxins such as the diphtheria toxin T domain or the pore domains of colicins (Choe et al. 1992; Parker et al. 1992).

The close structural similarity between Bcl-x_L and channel-forming bacterial toxins suggested early on that Bcl-2 family proteins are able to form pores in lipid bilayers (Muchmore et al. 1996). Consequently the channel-forming properties of Bcl-x_L, Bcl-2 and Bax have been characterised in vesicle efflux and single-channel measurements (Antonsson et al. 1997; Minn et al. 1997; Schendel et al. 1997; Schlesinger et al. 1997). The Bcl-x_L-ΔC (i.e. lacking C terminal hydrophobic helix) (Minn et al. 1997) and Bcl-2-ΔC channels (Schendel et al. 1997) resemble those of colicins in that they are discrete, cation-selective and pH-dependent. In contrast, the permeability changes induced in planar lipid bilayers by Bax are arbitrary and continuously variable (Basanez et al. 1999). Bax also exhibits lytic activities against neuronal or red blood cells as well as releasing fluorescent dyes from liposomes (Antonsson et al. 1997). Interestingly, these membrane-directed activities of Bax can be inactivated by ≥equimolar amounts of Bcl-2 (Antonsson et al. 1997).

The anti-apoptotic function of Bcl-2 has been suggested either as a direct neutralising interaction with Bax (Antonsson et al. 1997; Priault et al. 1999) or due to a Bcl-2 dependent hyperpolarization of mitochondrial membranes (Schendel et al. 1998). In both cases this organelle is protected from the detrimental 'mitochondrial permeability transition' (Kluck et al. 1997; Zamzami et al. 1996; Zoratti and Szabo 1995). Membrane-association of Bcl-2 proteins is therefore important to facilitate the interactions between the various players in controlled cell death (Häcker and Vaux 1995). Although, high-resolution structural data have been obtained for Bcl-2 family members and colicins in crystalline or aqueous environments (Muchmore et al. 1996; Parker et al. 1992; Vetter et al. 1998), much less is known about the structure and interactions of these proteins in the presence of membranes.

Solution NMR studies in membrane mimetic environments indicate that the tertiary structure of the C-terminally truncated Bcl-x_L protein (Bcl-x_L-ΔC) completely unfolds once the detergent exceeds the critical micelle concentration (cmc) (Losonczi et al. 2000). However, the protein remains composed of several α-helices separated by flexible loops (Fig. 1a). CD- and solution NMR-spectroscopy indicate a similarly high helix content after insertion into micelles (Losonczi et al. 2000).

Previous biophysical investigations of Bcl-x_L-ΔC in the presence of phospholipid bilayers have resulted in two opposing models of this protein at neutral pH. Whereas Marassi and co-workers using solid-state NMR spectroscopy suggest transmembrane insertion of helices 5 and 6 (Franzin et al. 2004), Blake and co-workers using optical spectroscopy and differential scanning calorimetry find no evidence for membrane insertion of Bcl-x_L-ΔC (Thuduppathy et al. 2006). Their model therefore suggests that insertion of the hairpin encompassing helices 5 and 6 requires acidic conditions and that at physiological pH only the most C-terminal helix anchors the protein in the membrane. To clarify this issue we re-evaluated the membrane interactions of Bcl-x_L using a variety of biophysical techniques including surface plasmon resonance, fluorescence- and oriented solid-state NMR spectroscopies. Care was taken to avoid the usage of detergents during the reconstitution protocol.

Whereas structural analysis by multidimensional solution NMR-spectroscopy relies upon data obtained from highly mobile molecules in solution, solid-state NMR spectroscopic methods have to be applied to obtain information about the structure and dynamics of peptides which are associated with extended lipid bilayers [recent review (Bechinger et al. 2004)]. The anisotropic contributions of the chemical shift, the dipolar and the quadrupolar interactions constitute the most pronounced features of static solid-state NMR spectra. Notably, the magnitude and the orientational dependence of nuclear interactions provide valuable information about the dynamics, the molecular structure, and the alignment of peptides when associated with lipid bilayers. For example, when uniaxially oriented samples are investigated by proton-decoupled ^{15}N solid-state NMR spectroscopy the approximate tilt of backbone ^{15}N labelled helices is directly obtained from the ^{15}N chemical shift position (Bechinger and Sizun 2003). Whereas transmembrane helical peptides exhibit ^{15}N resonances >180 ppm, in-plane oriented peptides are characterised by chemical shifts <100 ppm (Fig. 3a). Combining information from several labelled sites thus has the potential for detailed structural and topological information on membrane-associated polypeptides (Aisenbrey and Bechinger 2004b; Cross 1997).

The potential of these approaches depends to a large extent on the availability of polypeptides labelled with stable isotopes suitable for NMR spectroscopic investigations. Whereas large proteins are best prepared by bacterial overexpression and biochemical purification methods, smaller polypeptides are in general prepared more easily by solid-phase peptide synthesis. Although the first method is well suited to introduce isotopic labels in a uniform or selective manner (all or a given type of residues), it has proven difficult to obtain the large quantities of Bcl-x_L required for structural studies. The problem of large-scale bacterial expression has been solved by deletion of the hydrophobic C-terminus from the protein (ΔC) and many structural and functional studies have been performed using these truncated proteins (Muchmore et al. 1996). Notably, channel and anti-apoptotic activities of the protein persist after truncation of the C-terminus (Antonsson et al. 1997; Basanez et al. 1999; Minn et al. 1997; Muchmore et al. 1996).

Even though chemical synthesis of polypeptides is currently unsuitable for the production of large quantities of proteins of the size of the Bcl-x_L is has distinct advantages when smaller polypeptides labelled at a single or a few selected sites are required. In this paper both methods have been used in order to assemble a more complete and complementary view on the structure and topology of membrane-associated Bcl-x_L. In particular we have investigated if the physico-chemical properties of a peptide encompassing helices 5 and 6 allow the formation of a transmembrane helical loop after membrane association at neutral pH, as this domain has previously been suggested to form such an anchoring domain under acidic conditions (Thuduppathy et al. 2006; Thuduppathy and Hill 2006) or after exposure to detergents (Franzin et al. 2004). Furthermore, we have investigated the C-terminal domain of Bcl-x_L, which has been proposed to provide a first anchor of the protein in the membrane (Thuduppathy et al. 2006), although its membrane interactions have not been investigated experimentally.

Materials and methods

Expression and purification of Bcl-x_L

The Bcl-x_L protein was expressed in an *E. coli* BL21 DE3 (pLysE) strain transformed with the plasmid pTOLT-BCLXL as described previously (Anderluh et al. 2003). The DNA fragment encoding for BCL-XL was amplified by PCR using the following forward and reverse oligonucleotides, respectively, TTTTTTAGGCCTTCTCAGAGC AACCGGGAG and TTTTACGCGTTCATTTCCGACTG AAGAG, and introduced into the pTOLT plasmid using *Stu*I and *Mlu*I restriction sites. This plasmid was named as a pTOLT-BCLXL (Fig. 1) and DNA sequencing of this plasmid confirmed that the BCL-XL encoding DNA fragment was correctly inserted after the thrombin cleavage site on the pTOL vector. The bacteria were grown in minimal

media where the only nitrogen source was $^{15}NH_4^+$. During the exponential phase the cell cultures were induced for 3 h in the presence of IPTG after which the cells were harvested by centrifugation and lysed using a French press. The N-terminal 6X Histidine-tag facilitated purification of the Tol-BCL fusion by means of Ni-NTA affinity column. The expression and purification of the fusion protein was analysed by SDS-PAGE (supplementary Fig. S1) and the protein concentration determined by UV absorption at 280 nm. Bcl-x_L-ΔC was released by thrombin cleavage of the TolA-BCL fusion product and recovered by Ni-NTA affinity chromatography. The cleaved Bcl-x_L-ΔC contains an additional glycine and serine at the N-terminus from the thrombin cleavage site. MALDI Mass spectrometry confirmed the size of the truncated construct as 23,706 ± 3 Da (expected = 23,722.0 Da).

Peptide synthesis

The peptides Bcl-x_L-C and Bcl-xL-h5-h6 were prepared by solid-phase peptide synthesis on a Millipore 9050 or an Applied Biosystems 433A automatic peptide synthesiser using Fmoc (9-fluorenylmethyloxycarbonyl) chemistry (Atherton et al. 1981; Carpino and Han 1972). The Bcl-xL-h5-h6 peptide with the sequence RDGVNWGRIVAF FSFGGALCVESVDKEMQVLVSRIAAWMATYLNDHLE (cf. Fig. 1) was obtained on a TentaGel R PHB-Glu(t-Bu) resin (RAPP Polymer, Tübingen, Germany) when the standard synthetic protocols of this peptide synthesiser were applied. Notably, double couplings were used and non-reacted fragments were capped after each step by acetylation. Furthermore, the 'pseudo proline' technology was used at the F13-S14, D22-S23 and V32-S33 positions (Haack and Mutter 1992). The Fmoc-Phe-Ser(Ψ-Me, Me Pro)-OH, Fmoc-Glu(OtBu)-Ser(Ψ-Me, Me Pro)-OH, and Fmoc-Val-Ser(Ψ-Me, Me Pro)-OH were from Novabiochem, VWR International (Fontenay sous Bois, France). At positions 11 and 36 of Bcl-xL-h5-h6 (underlined in the sequence) the ^{15}N labelled derivative of alanine was inserted (Cambridge Isotopes Inc., Andover, MA, USA).

During the synthesis of the Bcl-x_L-C peptide (ERFNRWFLTGMTVAGVVLLGSL FSRK; cf. Fig. 1) a TentaGel R PHB-Gly Fmoc resin (RAPP Polymer, Tübingen, Germany) was used and double couplings were applied. The ^{15}N labelled derivative of alanine was inserted at the underlined position 14 (Cambridge Isotopes Inc., Andover, MA, USA). The synthetic products were purified by reverse phase high performance liquid chromatography using an acetonitrile/water gradient and a (218TP54, C18, 300 Å, 4.6 mm i.d., 250 mm) column (Vydac, France). The identity and purity of the synthesised peptides were analysed by using the matrix-assisted laser desorption ionisation mass spectrometry (MALDI-MS) and analytical reverse phase HPLC.

Sample preparation for solid-state NMR

The phospholipids 1-palmitoyl-2-oleoyl-*sn*-glycero-3-phosphocholine (POPC), 1,2-dioleoyl-*sn*-glycero-3-phosphocholine (DOPC) and 1-palmitoyl-2-oleoyl-*sn*-glycero-3-phospho-L-serine (POPS) were purchased from Avanti Polar Lipids (Alabaster, AL, USA), 1-palmitoyl-2-oleoyl-*sn*-glycero-3-[phospho-*rac*-(1-glycerol)] (POPG) from Sigma Aldrich (Lyon, France). In order to prepare oriented bilayers 10 mg Bcl-x_L-h5-h6 was dissolved in hexafluoroisopropanol and mixed with 150 mg DOPC/DOPG 70:30 mol/mol to yield a peptide-to-lipid molar ratio of 1% at neutral pH. The C-terminal hydrophobic peptide (6–11 mg) was co-dissolved in dichloromethane (or trifluoroethanol) together with the phospholipid at a concentration of 1 mol%. The lipid–peptide mixtures were applied onto 30 ultra-thin cover glasses (9 × 22 mm; Paul Marienfeld GmbH & Co. KG, Lauda-Königshofen, Germany), first dried in air and thereafter in high vacuum over night (1.8×10^{-2} mbar). The samples were equilibrated in a closed chamber where a defined relative humidity is obtained due to contact with saturated salt solutions of KNO_3 (93% r.h.), NH_4NO_3 (84% r.h.), NH_4Cl (75% r.h.), LiCl (15%), respectively (O'Brien 1948). After 3–5 days the glass plates were stacked on top of each other. The stacks were stabilised and sealed with teflon tape and plastic wrappings.

In order to reconstitute the biochemically prepared protein, 200 mg of POPC/POPS 70:30 mol:mol were co-dissolved in dichloromethane. The solvent was evaporated under a stream of nitrogen gas. The lipid film was suspended with 2 ml of double distilled water and the sample vortexed for several hours. Thereafter the suspension was extruded through a polycarbonate film with a pore size of 50 nm to obtain unilamellar vesicles. About 5 ml of protein stock solution (300 µg/ml protein in 20 mM phosphate buffer, 300 mM NaCl, 0.02% Sodiumazid) was added and the sample incubated for several hours. The sample was then concentrated using a Macrosep® 3 kD filter device (Pall, New York, USA). When ~1 ml of concentrate remained the sample was washed with 1 ml of water in order to reduce the salt concentration. The concentrated vesicle/protein suspension (~500 µl) was applied on 30 ultrathin coverplates (9 × 22 mm) and dried on air. The subsequent treatment including rehydration at 93% humidity was identical to samples containing synthetic peptides.

For *solid-state NMR spectroscopy* the samples were introduced into the flattened coils (Bechinger and Opella 1991) of a double-resonance probe and inserted into the magnetic field (9.4 T) of a Bruker Avance 400 wide-bore solid-state NMR spectrometer. The bilayers were oriented with the membrane normal parallel to the B_o field of the spectrometer, except where indicated otherwise. Proton-decoupled ^{15}N solid-state NMR spectra were acquired

using the MOIST cross-polarization pulse sequence (Levitt et al. 1986). The static solid-state NMR spectra were acquired typically using the following parameters: ^{1}H B_1 field of approximately 40 kHz, 1.3 ms contact time, 3 s recycle delay, spectral width: 40 kHz, 256 data points, number of acquisitions: 40,000. During acquisition the sample was cooled with a stream of air at room temperature. An exponential apodisation function corresponding to a line-broadening of 200 Hz was applied before Fourier transformation (except for Fig. 3b where the line-broadening is 100 Hz). NH_4Cl (41.5 ppm) was used as a reference corresponding to approximately 0 ppm for liquid NH_3.

The *fluorescence titration experiments* were performed as previously described (Sattler et al. 1997). The peptide representing the Bak BH3 domain (TKGQVGRQLAIIGDDINRRY) was added in a step-wise manner to 5 mM Bcl-x_L^{1-209} either in the absence or in the presence of 1.3 mM POPC/POPS 2:1 unilamellar vesicles (prepared by extrusion through 100 nm filters). The resulting change in the Bcl-x_L tryptophan fluorescence due to the association of peptide was monitored using a commercial spectrofluorometer (AMINCO-Bowman Series 2). The excitation wavelength was adjusted to $\lambda_{exc.} = 290$ nm while the emission wavelength was tuned from $\lambda_{fluo.} = 300$ to 400 nm at constant speed $S = 2$ nm/s. The excitation and the emission bandwidth were adjusted to $\Delta\lambda_{exc.} = \Delta\lambda_{fluo.} = 4$ nm.

Results and discussion

Helices of Bcl-x_L-ΔC are oriented parallel to the membrane surface

Uniformly labelled Bcl-x_L-ΔC (Bcl-x_L^{1-209}) was prepared by a new bacterial overexpression system which first produces a pTol-Bcl-x_L-ΔC fusion protein (Anderluh et al. 2003). After purification and cleavage of the fusion, the Bcl-x_L-ΔC was reconstituted into oriented phospholipid bilayers. In a related manner aligned membranes were prepared containing synthetic Bcl-x_L polypeptides corresponding to either the deleted hydrophobic C-terminus or the helix 5-loop-helix 6 domains ^{15}N labelled at one or two selected sites, respectively (Fig. 1). The resulting samples were inserted into the NMR spectrometer with the transmembrane axis "parallel" to the magnetic field direction or in a 90° "tilted" arrangement.

Figure 2a shows a proton-decoupled ^{15}N solid-state NMR spectrum of Bcl-x_L-ΔC, labelled uniformly with ^{15}N, reconstituted into oriented POPC/POPS (2:1 mol/mol) membranes in the parallel orientation. Biological and membrane activities of Bcl-x_L or Bcl-2 have been demonstrated previously in lipid mixtures of similar composition, with comparatively little effect of the presence or absence of the C-terminus (Antonsson et al. 1997; Basanez et al. 1999; Minn et al. 1997). The spectrum reveals predominant signal intensities at ^{15}N chemical shifts $\leq$100 ppm indicative of amide protons within helices oriented parallel to the membrane surface (tilt angles $\geq$55°). Figure 2b shows a simulated ^{15}N solid-state NMR spectrum of uniformly labelled Bcl-x_L-ΔC and will be discussed in further detail later.

In this chemical shift range the isotropic (orientation independent) resonances of 12 arginine (74 and 90 ppm), six tryptophan (84 ppm), and five lysine side chains (36 ppm) are also expected. The resonances of amide residues that exhibit isotropic reorientation as well as the isotropic chemical shifts of ten glutamine and 11 asparagine side chains (116 ppm) occur in the 100–130 ppm chemical shift range. The signals >150 ppm contribute <10% of the overall intensity and include four histidine side chains whose isotropic resonances are expected at $\geq$170 ppm. However, it should be noted that the cross polarisation technique was applied to acquire the solid state NMR spectra. On the one hand this technique takes advantage of the strong dipolar interactions to transfer magnetisation from the ^{1}H to the ^{15}N, thereby much enhancing the signal intensity of slowly moving or immobilised sites, and thus allowing the acquisition of the ^{15}N spectra shown in about 24 h. On the other hand the dipolar couplings of mobile residues are diminished or missing meaning that these exhibit much reduced or no signal intensities (Aisenbrey et al. 2006).

When the sample is tilted by 90° so that transmembrane helices will be perpendicular to the magnetic field direction contributions from the isotropic amide signal intensities, as well as broad distributions from immobilised domains, are obtained (Fig. 2c). In contrast to the parallel orientation shown in Figs. 2a and 3, the spectra obtained from the "perpendicular" sample orientation are sensitive to the rotational diffusion rate around the membrane normal. A priori an in-plane oriented helix, which is free to diffuse around the membrane normal, adopts a wide variety of alignments relative to the magnetic field direction. As each alignment results in its own chemical shift position within the 60–230 ppm range a powder pattern line shape is obtained which reflects the circular distribution of alignments (Aisenbrey and Bechinger 2004a). In contrast, when diffusion is fast the chemical shift anisotropy is averaged and a mean value is obtained. Although a minor part of the intensities observed in Fig. 2c, e.g. at 110 ppm, are sharp and indicative of motional averaging, the spectrum is predominantly characterised by broad circular powder pattern line shapes covering the full ^{15}N chemical shift range. The data thereby indicate that when associated with membranes rotational diffusion of Bcl-x_L-ΔC is slow when compared to the chemical shift anisotropy (7 kHz at 9.4 T). This indicates that although the association of truncated Bcl-x_L with the

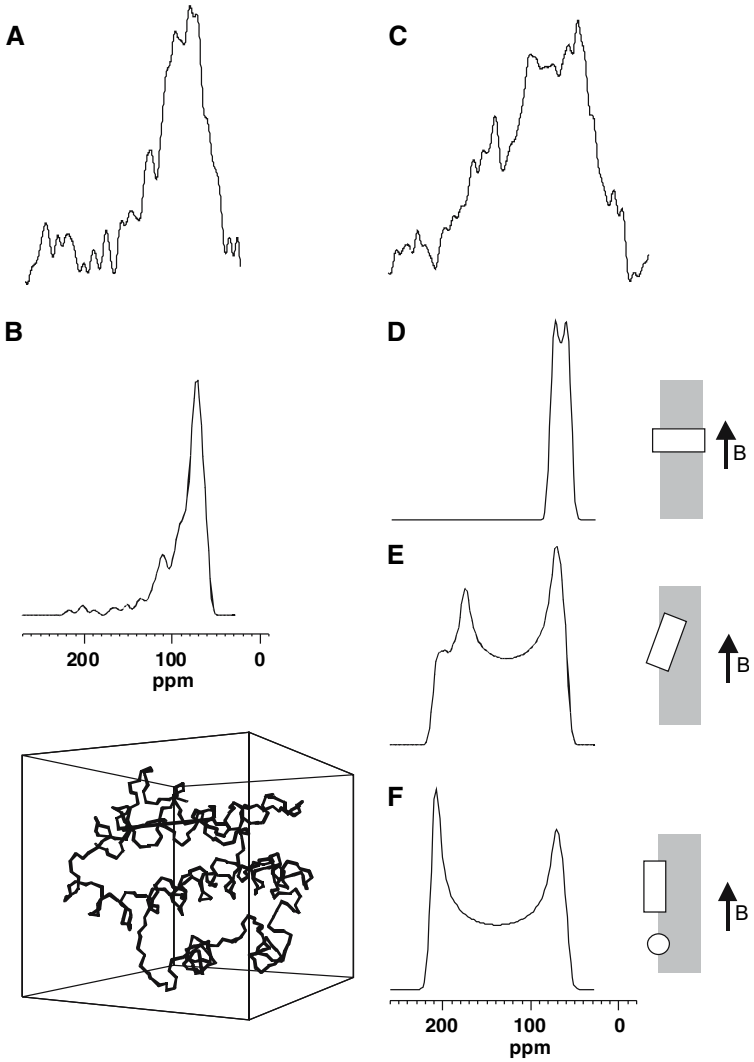

Fig. 2 Proton-decoupled ^{15}N solid-state NMR spectra of 1.5 mg uniformly labelled Bcl-x_L-ΔC (residues 1–209) reconstituted into 200 mg POPC/POPS 65/35 (wt./wt.) phospholipid bilayers oriented with their membrane normal parallel (**a**) and perpendicular (**c**) to the magnetic field direction (**B**). **b** Shows the simulated ^{15}N spectrum obtained when the PDB file 1BXL is oriented in the manner indicated. This is only one among a range of solutions where the helices are predominantly aligned parallel to the surface. **d–f** Simulations of ^{15}N chemical shift spectra of helices oriented at 0° (transmembrane), 70° or 90° (in-plane) relative to the membrane normal

membranes is weak (cf. below) it is enough to restrict protein diffusion.

For comparison, the spectral line shapes of the helical backbone signals for the tilted alignment have been simulated and are shown in Fig. 2d–f for helix tilt angles of 0° (transmembrane), 70° and 90° (perfect in-plane), respectively. Notably the simulations only represent immobile helix-backbone amides since the signal intensities of mobile amides or side chain nitrogens are weak or absent and have to be considered separately (cf. above). Although, the 70° spectral simulation shown in Fig. 2e already represents the most important features, the experimental result is more appropriately described by a linear combination of contributions from individual helices, mobile backbone residues with intensities in the 100–130 ppm range (signal intensity about 20%) and some residual side chain resonances (cf. above). Nevertheless, the comparison of the two orientations in Fig. 2 clearly indicates that the Bcl-x_L helices are oriented predominantly parallel to the membrane surface.

An isolated helix 5-loop-helix 6 does not insert in a transmembrane orientation

The helix 5-loop–helix 6 regions of several Bcl-2 proteins have been found to be particularly important for membrane association and biological activities (Garcia-Saez et al. 2004). We therefore investigated a 48-residue peptide encompassing the helix 5-loop–helix 6 domain of Bcl-x_L and obtained the proton-decoupled ^{15}N spectrum shown in Fig. 3b. Two isotopic labels were included in this peptide, one in the centre of each helix (Fig. 1a), therefore, the spectrum represents the sum of these two contributions. Clearly, the isolated domain might only partially represent the characteristics of the full-length protein (Garcia-Saez et al. 2004). Nevertheless, the ^{15}N chemical shift resonance at 80 ppm is incompatible with a stable transmembrane anchoring domain and confirms the observations obtained from the perlabelled protein shown in Fig. 2a where resonances corresponding to transmembrane helices are absent. The data thereby also explain the low membrane affinity of

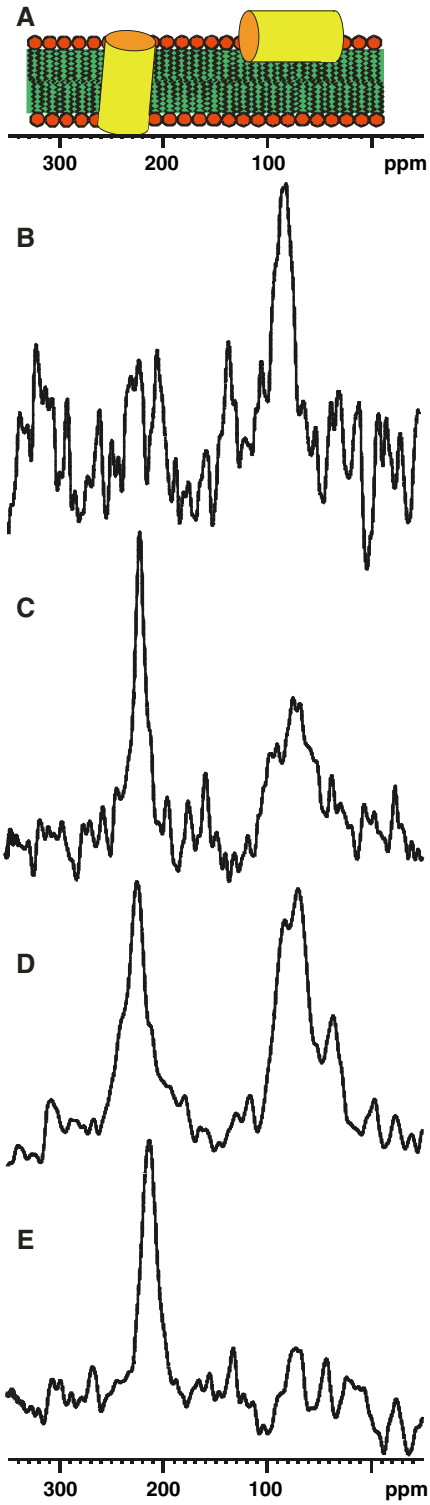

Fig. 3 **a** In membrane samples oriented with the bilayer normal parallel to the magnetic field direction the helix alignment correlates with the ^{15}N chemical shift position (cf. text for details). **b** Proton-decoupled ^{15}N solid-state NMR spectra of the Bcl-x_L h5-l-h6 domain labelled with ^{15}N at alanine-11 and alanine-36, and reconstituted into oriented phospholipid bilayers, and **c** the C-terminus of Bcl-x_L labelled with ^{15}N at the single alanine-14 residue after reconstitution into oriented POPC/POPS 3:1 phospholipid bilayers and equilibrated at 93% r.h. **d** Sample C equilibrated at 15% r.h. E. [^{15}N-Ala14]-Bcl-x_L-C-terminus in POPC membranes

the Bcl-x_L-ΔC domain that has been recently observed in the dilute solutions (Thuduppathy et al. 2006). ^{31}P solid-state NMR spectra of phospholipid bilayers encompassing increasing amounts of helix5-loop–helix6 polypeptide are shown in supplementary Fig. S2a–d.

In contrast, the data disagree with previous models of Bcl-x_L where helices 5 and 6 are suggested to form a transmembrane helical loop with tilt angles of about 50° (Franzin et al. 2004). The published proton-decoupled ^{15}N solid-state NMR spectrum of Bcl-x_L-ΔC exhibits additional signal intensities at about 170 ppm which were assigned to tilted backbone ^{15}N amides (Franzin et al. 2004). We have therefore simulated the ^{15}N solid-state NMR spectrum of Bcl-x_L-ΔC assuming that 40 residues adopt a 50° tilted alignment (supplementary Fig. S3). Clearly, the strong intensities in the 170–180 ppm region, that are characteristic for this structural arrangement, are absent in our experimental spectrum.

We have previously observed signal intensities in the 170 ppm range when working with His-tagged proteins (Prongidi Fix 2005) in agreement with known side chain chemical shift assignments. This may be important since in contrast to the previous work (Franzin et al. 2004; Prongidi Fix 2005) the 6-His tag was removed from our Bcl-x_L protein preparation. Another important difference derives from the use of detergent in previous Bcl-x_L reconstitution protocols (Franzin et al. 2004) which might have promoted the unfolding of the protein (Losonczi et al. 2000).

The C-terminal helix adopts a largely transmembrane orientation

When a polypeptide corresponding to the C-terminal helix of Bcl-x_L, Bcl-$x_L^{208–233}$ labelled with ^{15}N at its centre, was reconstituted into oriented POPC/POPS 2:1 membranes a chemical shift of 221 ppm was observed (Fig. 3c). This value agrees perfectly with the suggested transmembrane α-helix insertion of this domain (Losonczi et al. 2000). However, an additional broad signal intensity is observed in Fig. 3c with a maximum at 74 ppm. This signal was enhanced when the sample is equilibrated at reduced relative humidity (Fig. 3d). At the same time the ^{31}P NMR spectra remained indicative of well-oriented phospholipid bilayers (cf. supplementary Fig. S2e). The occurrence of two ^{15}N signal intensities indicates a topological or conformational equilibrium, in which, to cite one possibility, transmembrane and in-plane oriented helices are in slow exchange. This behaviour is consistent with a considerable hydrophobic moment of this α-helix within an overall hydrophobic character. In the absence of POPS the spectrum of Bcl-$x_L^{208–233}$ exhibits a chemical shift of 213 ppm indicative of only small changes in tilt angle and/or dynamics upon modification of the lipid composition (Fig. 3e).

Structural model of membrane-associated Bcl-x_L at physiological pH

The structural models shown in Fig. 4 summarise the data presented in this paper. Whereas the recombinant protein encompassing helices 1–8 exhibits predominant in-plane orientations (Figs. 2a; 3b) the extreme C-terminal polypeptide adopts a predominantly transmembrane alignment (Fig. 3c–e). Figure 4a schematically represents such a structure. The ^{15}N spectrum of the 90° tilted sample of Bcl-x_L-ΔC indicates that about 80% of the signal intensities exhibit rotational correlation times that are slow on the time scale of the ^{15}N chemical shift measurement (Fig. 2c) and is indicative for membrane-association of the proteins. In analogy to the fold that has been observed previously in micellar environments (Losonczi et al. 2000) the model shown in Fig. 4a shows an open and flexible structure of Bcl-x_L in a lipid bilayer where helices 1–8 exhibit planar alignments. However, the authors of this former study (Losonczi et al. 2000) have raised doubts about the biological significance of such an open structure as the micelle-associated protein is monomeric whereas Bcl-x_L forms multimers in lipid bilayers.

When the association of Bcl-x_L with POPC/POPS 2:1 vesicles was tested using isothermal titration calorimetry, centrifugation- or Biacore assays binding was weak in agreement with previous investigations (Thuduppathy et al. 2006). This binding data thereby support a more superficial association without the deep membrane insertion of hydrophobic domains, in contrast to suggestions made after studying the protein at low pH (Thuduppathy et al. 2006; Thuduppathy and Hill 2006), or after exposure to detergents (Franzin et al. 2004; Losonczi et al. 2000). In addition, the dissociation constant of the Bak BH3 domain was determined using a fluorescence assay (Sattler et al. 1997) and shown to be (0.17 ± 0.05 μM) and (0.28 ± 0.06 μM) in the presence or absence of POPC/POPS 2:1 unilamellar vesicles, respectively (Fig. 5). This data is in good agreement with previous investigations using related ligands (Muchmore et al. 1996) and favours structural models which leave the BH3 binding groove intact.

We, therefore, simulated the proton-decoupled ^{15}N solid-state NMR spectra that would result from the Bcl-x_L crystal structure (Muchmore et al. 1996) at different alignments relative to the membrane surface. When all possible orientations are screened a range of arrangements is identified in which most Bcl-x_L helices orient parallel to the membrane surface (Figs. 2b; 4b). As a consequence the corresponding ^{15}N solid state NMR spectra are virtually devoid of signal intensities >150 ppm (Fig. 2b), just as observed in the experimental NMR spectrum shown in Figs. 2a and S3. Although in this model Bcl-x_L-ΔC does not insert deeply in the membrane, weak interactions of the protein at the membrane surface are sufficient to align the protein in our sample preparations (Fig. 2a).

Structural investigations of Bcl-2 proteins suggest that peptides encompassing high-affinity BH3 domains bind to the same hydrophobic groove which in solution is occupied by the C-terminal hydrophobic sequence (Denisov et al. 2003; Hinds et al. 2003; Suzuki et al. 2000). The model shown in Fig. 4b preserves the possibility of Bcl-x_L interacting with other Bcl-2 proteins in its membrane-associated state. Furthermore, our data indicate that the C-terminus of Bcl-x_L inserts in a transmembrane fashion (Fig. 3c–e) supporting the idea that it acts as a membrane anchor (Kim et al. 2004; Thuduppathy et al. 2006). Whereas the Bcl-x_L C-terminus encompasses a continuous stretch of 18 hydrophobic residues, sufficiently long to span the hydrophobic bilayer, the hydrophobic regions of helices 5 and 6 are considerably shorter and, therefore, probably not suitable as transmembrane anchoring domains. In this manner membrane insertion of the C-terminus can at the same time expose the BH3-binding site. Therefore, membrane-insertion of Bcl-x_L and the possibility to oligomerise with other members of the family seem tightly connected processes.

The in-plane alignment of all but the most C-terminal helices is in good agreement with the anti-apoptotic activity of Bcl-x_L where membrane permeation of large molecules is absent (Basanez et al. 1999). Our data suggest a model in which upon membrane-association at physiological pH much of the helix–helix interactions within the protein are preserved in agreement with previous propositions

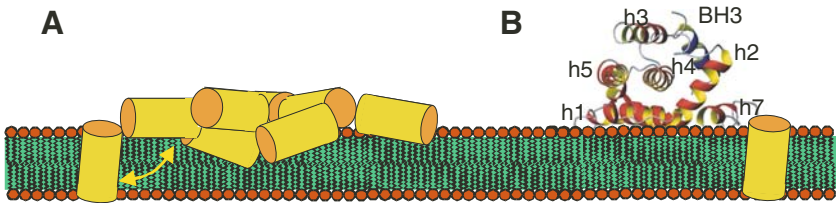

Fig. 4 Models for bilayer-associated Bcl-x_L. Our ^{15}N solid-state NMR experiments indicate an in-plane alignment of the first eight helices of the protein with only the C-terminal helix adopting a transmembrane alignment. Model A shows the topology in bilayers assuming that the protein completely unfolds. Model B is based on the PDB file 1BXL where the protein structure is preserved and oriented in such a manner to fit the experimental NMR spectrum (helices oriented parallel to the membrane surface). It remains possible that partial unfolding of the protein occurs

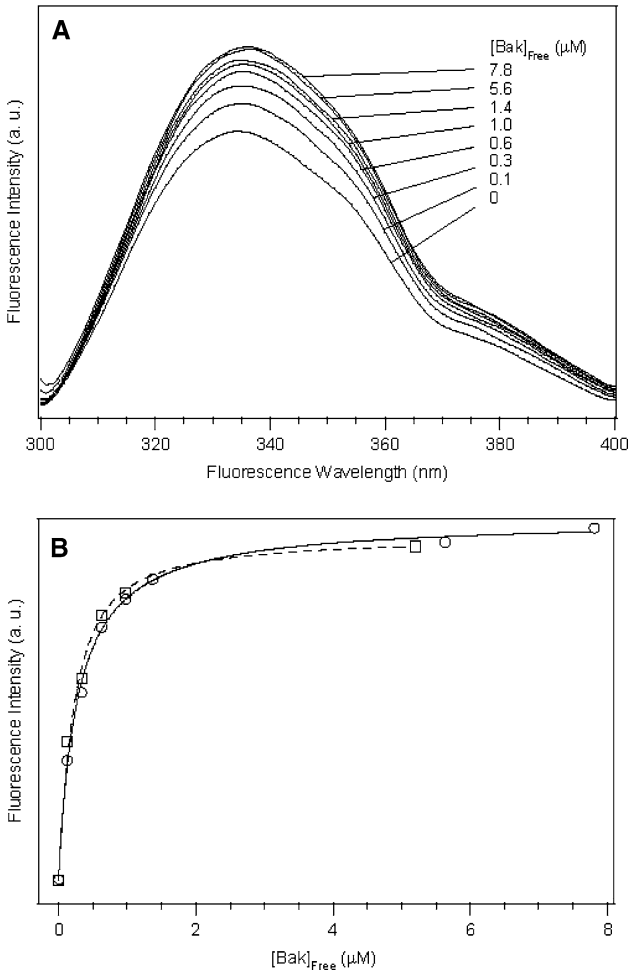

Fig. 5 **a** Fluorescence spectra obtained from the titration of increasing amounts of peptide representing the Bak BH3 domain (TKGQVGRQLAIIGDDINRRY) to 5 mM Bcl-x_L-ΔC. The relative integrated fluorescence intensities are shown in the absence (*solid line*, *circles*) and in the presence of 1.3 mM POPC/POPS 2:1 unilamellar vesicles (prepared by extrusion through 100 nm filters; *hatched line*, *squares*)

(Thuduppathy et al. 2006). At the same time the C-terminus assures targeting to and insertion into the membrane (Kaufmann et al. 2003). The accompanying conformational changes liberate the hydrophobic binding groove (Denisov et al. 2003; Hinds et al. 2003; Suzuki et al. 2000) which thereby becomes accessible for heterodimerisation. The spatio-temporal redistribution of proteins and the associated conformational changes can thus serve as key regulatory events during apoptosis.

Acknowledgments We are grateful to Gérard Nullans and Josefine März for their help during peptide synthesis. The work was funded by the Association pour la Recherche sur le Cancer (ARC) and the PPF RMN Grand-Est of the French Ministry of Research. We acknowledge the support by the Région Alsace and the Agence Nationale pour la Recherche contre le SIDA (ANRS) for initially helping the students with a fellowship (C.A. and S.U.S.).

References

Adams JM, Cory S (2001) Life-or-death decisions by the Bcl-2 protein family. Trends Biochem Sci 26:61–68

Aisenbrey C, Bechinger B (2004a) Investigations of peptide rotational diffusion in aligned membranes by 2H and 15N solid-state NMR spectroscopy. J Am Chem Soc 126:16676–16683

Aisenbrey C, Bechinger B (2004b) Tilt and rotational pitch angles of membrane-inserted polypeptides from combined 15N and 2H solid-state NMR spectroscopy. Biochemistry 43:10502–10512

Aisenbrey C, Harzer U, Bauer-Manz G, Bär G, Husmal Chotimah IN, Bertani P, Sizun C, Kuhn A, Bechinger B (2006) Proton-decoupled 15N and 31P solid-state NMR investigations of the Pf3 coat protein in oriented phospholipid bilayers. FEBS J 273:817–828

Anderluh G, Gokce I, Lakey JH (2003) Expression of proteins using the third domain of the *Escherichia coli* periplasmic-protein TolA as a fusion partner. Protein Expr Purif 28:173–181

Antonsson B, Contin F, Ciavatta A, Montesuit S, Elwis S, Marinou I, Bernasconi L, Bernard A, Mermod JJ, Mazzei G (1997) Inhibition of Bax channel-forming activity by Bcl-2. Science 277:370–372

Atherton E, Logan CJ, Sheppart RC (1981) Peptide synthesis: Part 2. Procedures for solid-phase synthesis using N^{α}-fluorenyllmethoxycarbonylamino-acids on polyamide supports. Synthesis of substance P and of acyl carrier proteins 65–74 decapeptide. J Chem Soc Perkin Trans I 538–546

Basanez G, Nechushtan A, Drozhinin O, Chanturiya A, Choe E, Tutt S, Wood KA, Hsu Y, Zimmerberg J, Youle RJ (1999) Bax, but not Bcl-xL, decreases the lifetime of planar phospholipid bilayer membranes at subnanomolar concentrations. Proc Natl Acad Sci USA 96:5492–5497

Bechinger B, Opella SJ (1991) Flat-coil probe for NMR spectroscopy of oriented membrane samples. J Magn Reson 95:585–588

Bechinger B, Sizun C (2003) Alignment and structural analysis of membrane polypeptides by 15N and 31P solid-state NMR spectroscopy. Concepts Magn Reson 18A:130–145

Bechinger B, Aisenbrey C, Bertani P (2004) Topology, structure and dynamics of membrane-associated peptides by solid-state NMR spectroscopy. Biochim Biophys Acta 1666:190–204

Borner C (2003) The Bcl-2 protein family: sensors and checkpoints for life-or-death decisions. Mol Immunol 39:615–647

Butler LM, Hewett PJ, Fitridge RA, Cowled PA (1999) Deregulation of apoptosis in colorectal carcinoma: theoretical and therapeutic implications. Aust N Z J Surg 69:88–94

Carpino LA, Han GY (1972) The 9-fluorenylmethoxycarbonylamino-protecting group. J Org Chem 37: 3404

Chao DT, Korsmeyer SJ (1998) BCL-2 family: regulators of cell death Ann Rev Immunol 16:395–419

Choe S, Bennett MJ, Fujii G, Curmi PM, Kantardjieff KA, Collier RJ, Eisenberg D (1992) The crystal structure of diphtheria toxin. Nature 357:216–222

Cross TA (1997) Solid-state nuclear magnetic resonance characterization of gramicidin channel structure. Meth Enzymol 289:672–696

Day CL, Chen L, Richardson SJ, Harrison PJ, Huang DC, Hinds MG (2005) Solution structure of prosurvival mcl-1 and characterization of its binding by proapoptotic bh3-only ligands. J Biol Chem 280:4738–4744

Denisov AY, Madiraju MS, Chen G, Khadir A, Beauparlant P, Attardo G, Shore GC, Gehring K (2003) Solution structure of human BCL-w: modulation of ligand binding by the C-terminal helix. J Biol Chem 278:21124–21128

Franzin CM, Choi J, Zhai D, Reed JC, Marassi FM (2004) Structural studies of apoptosis and ion transport regulatory proteins in membranes. Magn Reson Chem 42:172–179

Garcia-Saez AJ, Mingarro I, Perez-Paya E, Salgado J (2004) Membrane-insertion fragments of Bcl-xL, Bax, and Bid. Biochemistry 43:10930–10943

Haack T, Mutter M (1992) Serine derived oxazolidines as secondary structure disrupting, solubilizing building blocks in peptide synthesis. Tetrahedron Lett 33:1589–1592

Häcker G, Vaux DL (1995) Apoptosis: a sticky business. Curr Biol 5:622–624

Hinds MG, Lackmann M, Skea GL, Harrison PJ, Huang DC, Day CL (2003) The structure of Bcl-w reveals a role for the C-terminal residues in modulating biological activity. EMBO J 22:1497–1507

Huang Q, Petros AM, Virgin HW, Fesik SW, Olejniczak ET (2002) Solution structure of a Bcl-2 homolog from Kaposi sarcoma virus. Proc Natl Acad Sci USA 99:3428–3433

Huang Q, Petros AM, Virgin HW, Fesik SW, Olejniczak ET (2003) Solution structure of the BHRF1 protein from Epstein–Barr virus, a homolog of human Bcl-2. J Mol Biol 332:1123–1130

Kaufmann T, Schlipf S, Sanz J, Neubert K, Stein R, Borner C (2003) Characterization of the signal that directs Bcl-x(L), but not Bcl-2, to the mitochondrial outer membrane. J Cell Biol 160:53–64

Kim PK, Annis MG, Dlugosz PJ, Leber B, Andrews DW (2004) During apoptosis bcl-2 changes membrane topology at both the endoplasmic reticulum and mitochondria. Mol Cell 14:523–529

Kluck RM, Bossy-Wetzel E, Green DR, Newmeyer DD (1997) The release of cytochrome *c* friom mitochondria: a primary site for Bcl-2 regulation of apoptosis. Science 275:1132–1136

Levitt MH, Suter D, Ernst RR (1986) Spin dynamics and thermodynamics in solid-state NMR cross polarization J Chem Phys 84:4243–4255

Losonczi JA, Olejniczak ET, Betz SF, Harlan JE, Mack J, Fesik SW (2000) NMR studies of the anti-apoptotic protein Bcl-x(L) in micelles. Biochemistry 39:11024–11033

Merry DE, Korsmeyer SJ (1997) Bcl-2 gene family in the nervous system. Annu Rev Neurosci 20:245–267

Minn AJ, Vélez P, Schendel SL, Liang H, Muchmore SW, Fesik SW, Fill M, Thompson CB (1997) Bcl-X_L forms an ion channel in synthetic lipid membranes. Nature 385:353–357

Muchmore SW, Sattler M, Liang H, Meadows RP, Harlan JE, Yoon HS, Nettesheim D, Chang BS, Thompson CB, Wong SL, Ng SL, Fesik SW (1996) X-ray and NMR structure of human Bcl-xL, an inhibitor of programmed cell death. Nature 381:335–341

O'Brien FEM (1948) The control of humidity by saturated salt solutions. J Sci Instr 25:73–76

Parker MW, Postma JP, Pattus F, Tucker AD, Tsernoglou D (1992) Refined structure of the pore-forming domain of colicin A at 2.4 A resolution. J Mol Biol 224:639–657

Petros AM, Olejniczak ET, Fesik SW (2004) Structural biology of the Bcl-2 family of proteins. Biochim Biophys Acta 1644:83–94

Phillips AJ, Crowe JD, Ramsdale M (2006) Ras pathway signaling accelerates programmed cell death in the pathogenic fungus *Candida albicans*. Proc Natl Acad Sci USA 103:726–731

Priault M, Camougrand N, Chaudhuri B, Manon S (1999) Role of the C-terminal domain of Bax and Bcl-XL in their localization and function in yeast cells. FEBS Lett 443:225–228

Prongidi Fix L (2005) Structural and thermodynamic investigations of membrane-associated polypeptides and peptide/DNA transfection complexes. Ph.D thesis, University Louis Pasteur Strasbourg

Sattler M, Liang H, Nettesheim D, Meadows RP, Harlan JE, Eberstadt M, Yoon HS, Shuker SB, Chang BS, Minn AJ, Thompson CB, Fesik SW (1997) Structure of Bcl-xL-Bak peptide complex: recognition between regulators of apoptosis. Science 275:983–986

Schendel SL, Xie Z, Montal MO, Matsuyama SMMRJC (1997) Channel-formation by anti-apoptotic protein Bcl-2. Proc Natl Acad Sci USA 93:5113–5118

Schendel SL, Montal M, Reed JC (1998) Bcl-2 family proteins as ion-channels. Cell Death Differ 5:372–380

Schlesinger PH, Gross A, Yin X-M, Yamamoto K, Saito M, Waksman G, Korsmeyer SJ (1997) Comparison of the ion-channel characteristics of proapototic Bax and antiapoptotic Bcl-2. Proc Natl Acad Sci USA 94:11357–11362

Suzuki M, Youle RJ, Tjandra N (2000) Structure of Bax: coregulation of dimer formation and intracellular localization. Cell 103:645–654

Thuduppathy GR, Hill RB (2006) Acid destabilization of the solution conformation of Bcl-xL does not drive its pH-dependent insertion into membranes. Protein Sci 15:248–257

Thuduppathy GR, Craig JW, Kholodenko V, Schon A, Hill RB (2006) Evidence that membrane insertion of the cytosolic domain of Bcl-x(L) is governed by an electrostatic mechanism. J Mol Biol 359:1045–1058

Vetter IR, Parker MW, Tucker AD, Lakey JH, Pattus F, Tsernoglou D (1998) Crystal structure of a colicin N fragment suggests a model for toxicity. Structure 6:863–874

Zamzami N, Susin SA, Marchetti P, Hirsch T, Gomez-Monterrey I, Castedo M, Kroemer G (1996) Mitochondrial control of nuclear apoptosis. J Exp Med 183:1533–1544

Zoratti M, Szabo I (1995) The mitochondrail permeability transition. Biochim Biophys Acta 1241:139–176